Soil Gas Sampling and Analysis in Petroleum-Contaminated Transportation Department Right of Way

DAVID W. OSTENDORF, ALAN J. LUTENEGGER, AND SAMUEL J. POLLOCK

The lateral distribution, approximate composition, and aerobic biodegradation potential of vapors from a petroleum hydrocarbon spill in a Massachusetts Highway Department right of way was inferred from soil gas sampling technology and analyses. Stainless steel vapor probes were driven into the heterogeneous, nonuniform, contaminated sand of the right of way by a drill rig–mounted hammer. Stainless steel tubing clusters with sintered stainless steel filters were installed at selected locations in the right of way as well. A metered vacuum pump transferred soil gas from the probes and clusters into Tedlar bags for on-site analysis by a combustible hydrocarbon meter, an oxygen analyzer, and a portable gas chromatograph. Floating product from existing monitoring wells was brought to the laboratory for headspace analysis by gas chromatograph/mass spectrometer to identify the hydrocarbon vapor constituents and estimate the saturated vapor pressure. This headspace sample was used to calibrate the portable gas chromatograph and integrate the meter readings and chromatograms into a common hydrocarbon data base used to delineate the horizontal extent of the petroleum spill. The observed oxygen levels were input to a simple coupled transport model that confirmed the aerobic biodegradation potential of naturally occurring microbes in the site soil.

University of Massachusetts (UMASS) and Massachusetts Highway Department (MHD) researchers used soil gas sampling technology and analysis to estimate the lateral distribution, approximate composition, and aerobic biodegradation potential of petroleum hydrocarbon vapors from leaking storage tanks. The spill was in the right of way of State Route 128/Interstate 95 in Lexington, Massachusetts, about 600 m upgradient from a reservoir in the capillary fringe of the unconfined aquifer about 2.5 m below the ground surface.

SOIL GAS SAMPLING TECHNOLOGY

Soil gas sampling has proved to be a useful means of delineating the areal extent of gasoline (*1*), diesel fuel (*2*), heating oil (*3*), and other light petroleum distillate spills beneath the ground surface. These immiscible hydrocarbons are lighter than water and so spread out over the water table. Evaporation is a preferential transport mechanism because the contaminants are volatile, giving rise to elevated concentrations of hydrocarbon vapors in the soil gas above the separate phase hydrocarbons. Thus, soil gas surveys may be used to delineate the separate phase source of petroleum contamination.

D. W. Ostendorf and A. J. Lutenegger, Civil and Environmental Engineering Department, University of Massachusetts, Amherst, Mass. 01003. S. J. Pollock, Research and Materials Section, Massachusetts Highway Department, 400 D Street, South Boston, Mass. 02210.

Soil gas sampling works best in dry, coarse-grained soils with low organic carbon content (*4*). Infiltrating water, perched water tables, low-permeability lenses, barometric pressure fluctuations, lower soil temperatures, and biodegradation can all significantly reduce hydrocarbon vapor concentrations with increasing distance from the separate phase source. The infiltrating water, barometric pressure, and soil temperature effects are transient and can introduce seasonal or diurnal variations in gaseous contamination (*1,5*), so that frequent sampling from a permanent soil gas monitoring point is needed for a quantitative measure of contamination. Aerobic biodegradation of hydrocarbon vapors consumes oxygen (*6*) and generates carbon dioxide (*7*), whereas anaerobic degradation creates methane gas (*8*). The correlation of these constituents with an inert tracer gas is used to assess the biodegradation potential of petroleum spills in the subsurface environment (*9,10*).

A suite of increasingly sophisticated technologies is available for sampling and analyzing soil gas. Probes as simple as a 1.3-cm-diameter stainless steel tube tipped with a loose carriage bolt (*11*) or a drive point (*1*) have been deployed successfully in the field, as have more elaborate 2.0-cm-diameter stainless steel systems with side ports (*12*) or retractable shields (*13*). The driving force may be a manual or handheld electric hammer (*11,12*), truck-mounted piston (*14*), or a drill rig–mounted hammer, depending on the type of soil and sampling depth. Shields or filter elements may be required for finer-grained soils to prevent clogging of ports. Soil gas is pulled from the probes through stainless steel or flexible tubing to the ground surface by manual (*12*) or electric vacuum sampling pumps, where it can be trapped for subsequent laboratory analysis (*15*), subsampled by syringes (*12*), or fed directly into field meters (*11*). Organic vapor analyzers with built-in vacuum pumps and catalytic combustion chambers are used to measure total hydrocarbon vapor pressures, whereas potentiometric cells and infrared absorption sensors also see widespread use for detecting oxygen and carbon dioxide content, respectively. Tedlar bag dilution may be needed for field meter readings of highly contaminated soil gas (*16*). Petroleum distillates are blends of many hydrocarbon compounds with varying saturated vapor pressures, solubilities, and biodegradation potentials (*17*), and a catalytic combustion chamber does not differentiate constituents. Soil gas consequently is analyzed by direct injection or trap desorption into portable or mobile gas chromatographs to elucidate its hydrocarbon composition.

Elements of this existing technology were incorporated into the present study, which featured new developments as well. Durable vapor probes of simple design and rugged construction were designed and fabricated by UMASS investigators for deployment with electric and rig-driven hammers into relatively dense soil. Commercially available soil gas meters were used with a field gas

chromatograph and a laboratory gas chromatograph/mass spectrometer (gc/ms) analysis to yield calibrated estimates of total hydrocarbon vapor pressures. These data were combined with oxygen measurements in a coupled mathematical analysis of natural biodegradation in the unsaturated zone as an assessment of remediation potential at the site.

SITE CHARACTERIZATION

The study site is the parking lot of a service area (Figure 1), located on SR-128/I-95 northbound in Lexington and owned by MHD. More than 160,000 vehicles a day travel SR-128/I-95 in Lexington on six lanes of traffic. The highway borders an ephemeral stream that flows about 600 m south to a reservoir that serves as a surface drinking water source. An access road runs between the northbound travel lanes and the service area, and a grass strip separates this access road from the parking lot. The grass strip forms the downgradient boundary of the study area. The site is underlain by crystalline bedrock about 8.5 m below the ground surface, with a westward sloping water table that varies seasonally from 2 to 3 m below the ground surface.

UMASS efforts focused on the unsaturated zone, which consists of heterogeneous, nonuniform sands with considerable fine and gravel fractions. An array of Omega thermocouple leads was installed on 15.2-cm intervals tied to a PVC riser pipe installed down a borehole in the grass strip to measure soil temperature, T (Figure 1). The leads were read with an Omega Model HH21 handheld thermometer; depth-averaged temperatures of 281.0 and 282.2°K were read on December 28, 1993, and May 13, 1994, respectively. Gravimetric moisture contents were measured in soil borings taken by UMASS during drilling operations in July 1993; data below the water table implied an average volumetric porosity of 0.37, and near surface observations suggested an irreducible moisture content of 0.079. Thus the depth-averaged air porosity θ_A was 0.291.

The service area began operation as a restaurant with a gasoline and diesel filling station in 1954 (*18*), coincident with completion of road improvements to its present configuration. The complex is serviced by municipal water, sewer, and electrical utilities and is heated by fuel oil. The original service area included single-walled steel underground tanks for storing gasoline (seven tanks), diesel fuel (two tanks), heating oil (one tank), and waste oil (one tank), with approximate locations shown in Figure 1 (*bottom*). MHD engineers conducted an environmental site assessment in 1987 (*19*) and found liquid petroleum in two of four monitoring wells. All 11 original tanks were pulled in 1988 and replaced with new double-walled steel underground storage tanks for gasoline and diesel fuel and an above-ground heating oil tank [Figure 1 (*bottom*)]. MHD engineers installed 21 additional monitoring wells and 3 product recovery wells as part of a remediation system that operated from 1988 to 1991 (*20*). Separate phase petroleum hydrocarbons persisted in five of the monitoring wells, with episodic occurrences in two others. Spill masses were found under the service area parking lot and under the access road. The oil recovery system removed 1.93 m^3 of separate phase petroleum until its closure in June 1991 due in part to biofouling and corrosion (*21*). UMASS gauging in June 1994 confirmed persistent separate phase contamination in the five wells: three under the access road spill and two under the parking lot spill. The latter contamination is the focus of this paper.

SAMPLING AND ANALYTICAL METHODS

UMASS researchers mapped the lateral extent of total hydrocarbon and oxygen vapor pressures in the service area parking lot with stainless steel vapor probes on field trips in December 1993 and June 1994. Two different probes were designed, fabricated, and deployed by UMASS personnel (Figure 2). A 140-lb SPT rig-mounted safety hammer drove a retractable probe of 3.82-cm diameter with a 5.09-cm-diameter friction reducer and a flush-mounted shield through dirtier, more compacted soils to a depth of nearly 3 m. Cleaner, compacted soils were sampled successfully to a similar depth by a rig-driven probe equipped with a high-density polyethylene filter in place of the retractable sleeve. Both probes admitted soil gas through four 3.18-mm-diameter ports to a plenum connected to flexible Nalgene tubing routed to the surface through the rod annulus. A generator powered, Cole Parmer Model 7530-40 single-head diaphragm vacuum pump equipped with a water trap and Cole Parmer 0-5 L/min adjustable flow meter pulled soil gas to the surface. Larger 6.36-mm-diameter tubing and a 1-L purge volume were used in winter sampling to minimize vacuum-induced icing, and 3.18-mm-diameter tubing was used in spring sampling to minimize purging requirements. A 6.36-mm-diameter Nalgene line transferred 2 L of soil gas to Tedlar bags. A drop in gas flow registered by the flow meter signaled the onset of water clogging drawn from the capillary fringe and effectively stopped profiling at a given location.

The total hydrocarbon vapor pressure was measured by connecting the Tedlar bag to a battery-powered Bacharach TLV combustible hydrocarbon meter calibrated with hexane to a vapor pressure, p_V, of 500 parts per million (ppm). The meter had three scales to a maximum capacity of 10,000 ppm. A 2-L/min pump built into the meter pulled gas from the Tedlar bag through the inline filter into a catalytic combustion chamber for destructive sampling of the flow. The catalytic combustion required sufficient oxygen for meter accuracy, so that pressures were underpredicted for oxygen vapor pressures (p_{VO}) below 5 percent. Relative humidity and, to some extent, molecular weight of the hydrocarbons may have also introduced error into the readings (*16*). The oxygen partial pressure of the soil gas in the Tedlar bag was measured by a Bacharach Model 302 meter equipped with a potentiometric cell and a 2-L/min pump. The meter was calibrated with ambient air (presumed to be 20.9 percent oxygen) before and after each reading. A few heavily contaminated, low oxygen samples were diluted by injecting 0.50 L of soil gas into a second Tedlar bag, to which 1.5 L of compressed air was added (*1,16*). Thirty-nine depths at 8 paved locations were profiled using the drill rig on December 28, 1993, and 159 depths were sampled with the rig at 15 paved locations June 1–3, 1994.

Soil gas tubing clusters were installed in 19 boreholes drilled by 11.5-cm-diameter hollow-stem augers during field trips in October 1993, December 1993, and June 1994. The clusters consisted of 6.36-mm-diameter steel tubing cut in 0.50- or 1-m intervals to depths as great as 3 m (Figure 3). The tube ends were capped with 40-μm sintered stainless steel filters and set in a 2-mm-diameter sand pack with the augers raised slightly. Cuttings were backfilled into the borehole as the flight was pulled to the next cluster depth. Up to six tubes were emplaced in each cluster, which was finished with a cast iron cover set in concrete. The top of each tube was coupled to a Swagelok fitting to facilitate soil gas sampling. The Tedlar bag protocol was followed in the latter regard, with a Swagelok-equipped Nalgene transfer line coupling the cluster tube to the vacuum pump.

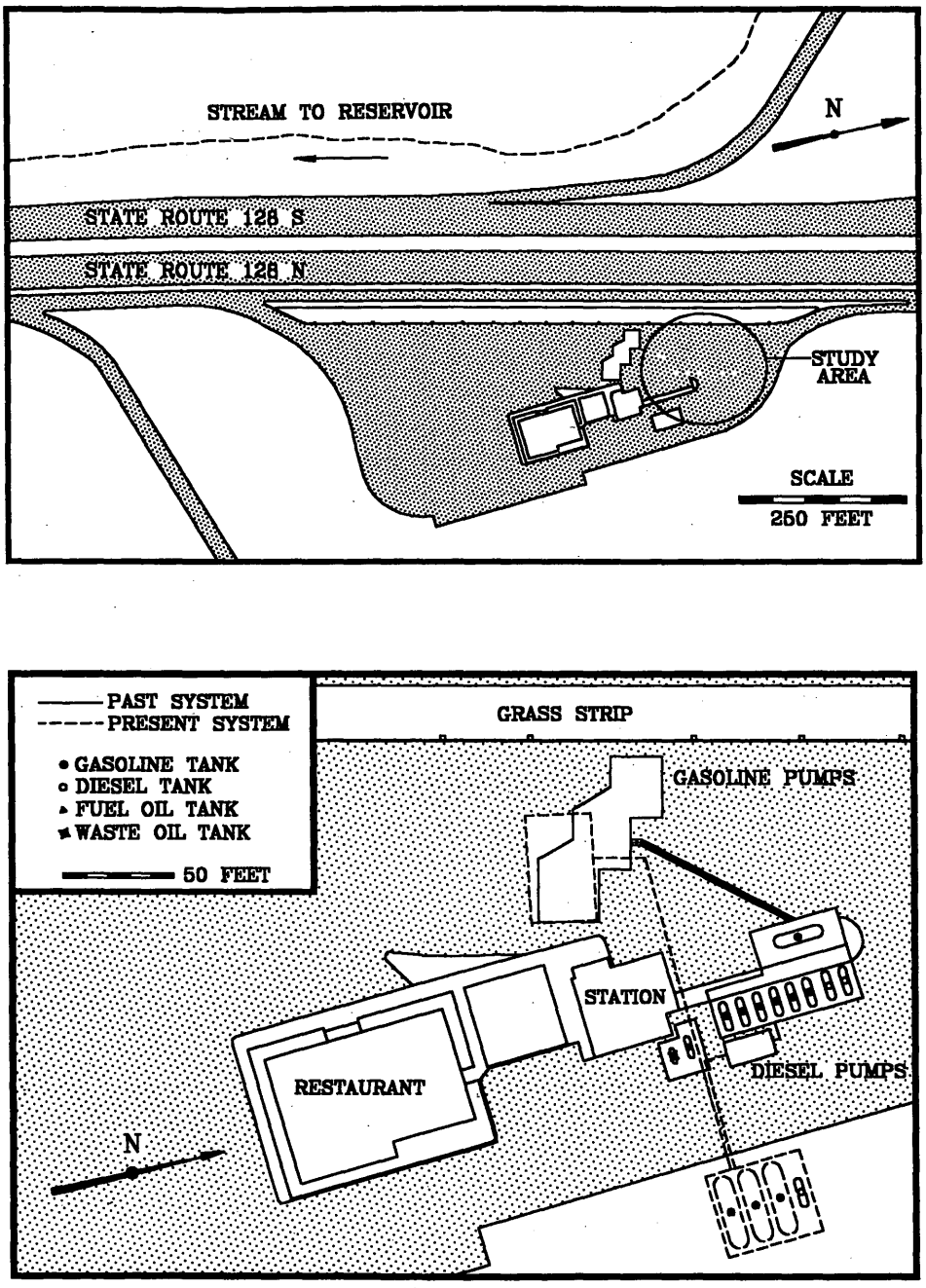

FIGURE 1 Location sketch: *top*, SR-128/I-95; *bottom*, service area.

Selected Tedlar bag samples were analyzed by gas chromatograph as well. A 250-μL Hamilton Gastight syringe with a 26-gauge bevel-tipped needle withdrew soil gas from the Tedlar bag for subsequent direct injection into an HNU System Model 311 portable gas chromatograph, equipped with a DB-5 capillary column of 0.53-mm diameter, 30-m length, and 0.5-μm film thickness. The injector and column temperatures were 200 and 50°C, respectively, and a 10-mL/min flow of research grade nitrogen carried the injection from the column to a 10.2 eV photoionization detector. The data were captured on HNU Peakworks software. Separate phase petroleum sampled from one of the MHD monitoring wells in May 1993 served as a standard for analysis. The standard was allowed to equilibrate with headspace in a 40-mL sample vial sealed with a Teflon-faced silicone septum.

APPROXIMATE COMPOSITION OF HYDROCARBON VAPORS

An analysis was performed on the UMASS Hewlett Packard 5898/5890 gc/ms to identify compounds and estimate the (saturated) vapor pressure of the headspace standard. Table 1 gives the 27 compounds in the headspace, obtained by matching observed electron impact spectra sensed by the gc/ms with library spectra.

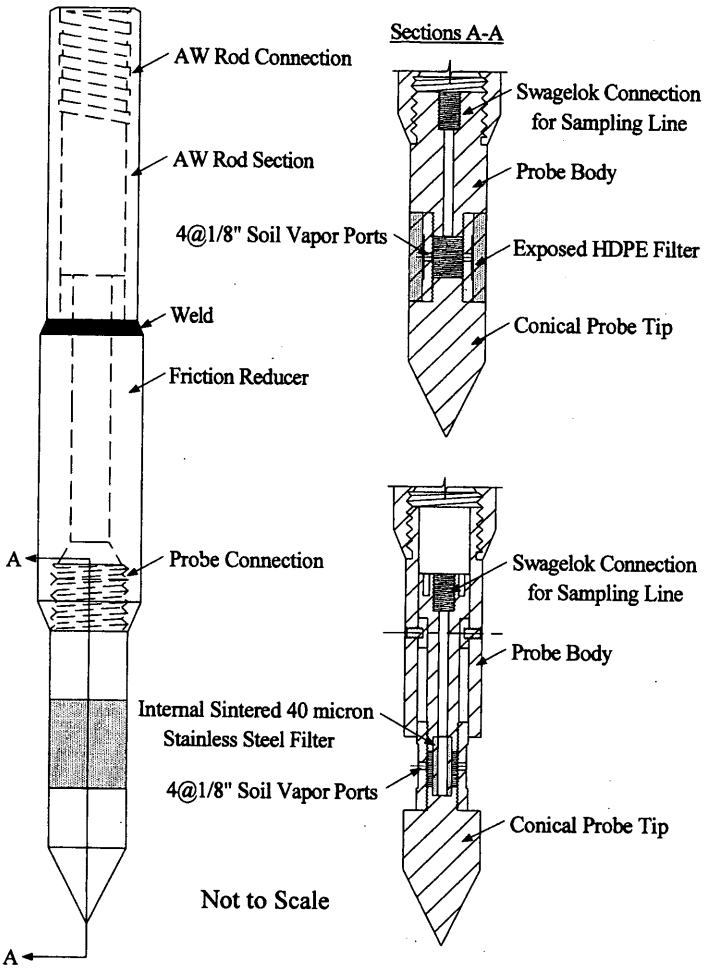

FIGURE 2 Stainless steel soil vapor probes with friction reducer and AW drill rod: *top*, HDPE filter probe; *bottom*, retractable probe with shield.

The vapors consisted primarily (93.7 percent) of alkanes with a small (6.3 percent) aromatic fraction. The most abundant compounds were 2 methylpentane (13.8 percent of the chromatographic area) and hexane (12.2 percent of the area). This composition was used to estimate the saturated vapor pressure of the standard, so that total hydrocarbon vapor pressures could be inferred from the chromatograms of the portable gc.

The saturated vapor pressure p_{VS} of the headspace is the sum of saturated partial pressures p_{VSI} of all the hydrocarbon constituents in equilibrium with the liquid petroleum in the sample vial

$$p_{VS} = \sum_I p_{VSI} \tag{1a}$$

$$p_{VSI} = p_{VSATI}\chi_I \tag{1b}$$

Equation 1b is Raoult's law (*22*) equating each compound's saturated partial pressure to the product of its mole fraction in the liquid petroleum in the sample vial χ_I and its saturated vapor pressure p_{VSATI} in equilibrium with pure liquid. Reid et al. (*23*) present an empirical equation for the latter parameter,

$$p_{VSATI} = p_C \exp\left(\frac{C_1\tau + C_2\tau^{1.5} + C_3\tau^3 + C_4\tau^6}{1-\tau}\right) \tag{2a}$$

$$\tau = 1 - \frac{T}{T_C} \tag{2b}$$

where

T = temperature (°K),
τ = relative temperature,
T_C = characteristic temperature,
p_C = characteristic pressure, and
C_N = coefficient tabulated for a large number of organic compounds.

The standard compounds given in Table 1 had computed 20°C saturated vapor pressures ranging from 1,300 to 760,000 ppm. The table presents the compounds by their elution order, which coincides closely with their volatility.

Equation 1 yielded an expression for the ratio ϵ_I of an individual constituent vapor pressure to the total vapor pressure under equilibrium conditions:

$$\epsilon_I = \frac{p_{VSI}}{p_{VS}} \tag{3a}$$

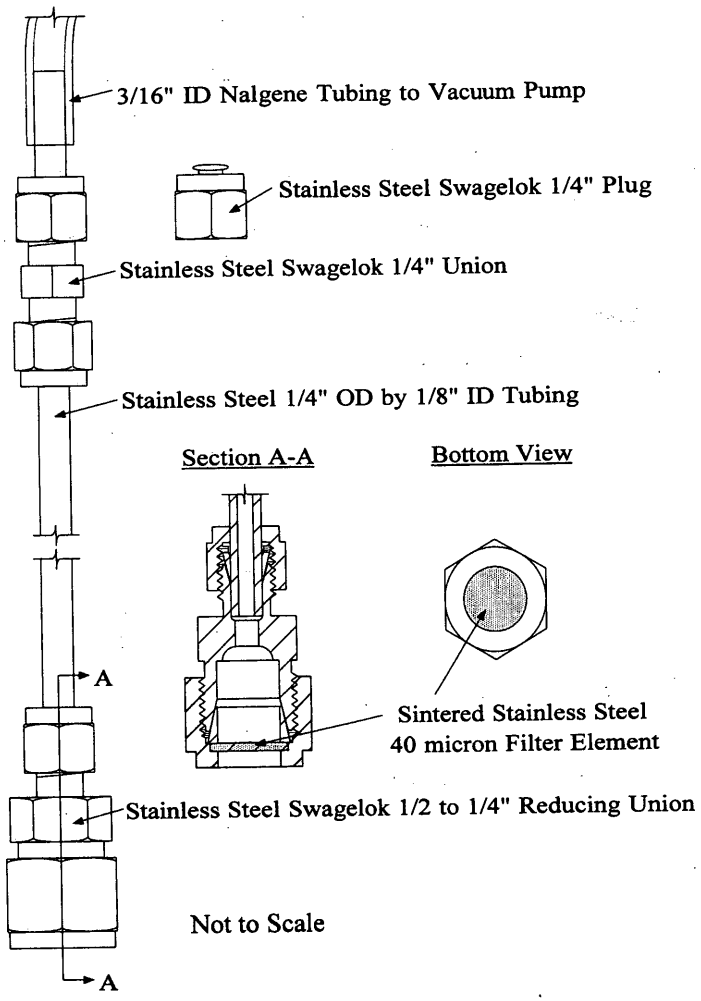

FIGURE 3 Stainless steel tubing cluster tube with sintered filter element and Swagelok coupling.

$$\epsilon_I = \frac{p_{VSATI}\chi_I}{\sum_I p_{VSATI}\chi_I} \tag{3b}$$

The ratio was assumed to be proportional to the reconstructed chromatographic area fraction A_I observed in the mass spectrometer, so that ϵ_I was known for each constituent (Table 1)

$$\epsilon_I = \frac{\left(\frac{A_I}{m_I}\right)}{\sum_I \frac{A_I}{m_I}} \tag{4}$$

with molar mass m_I for constituent I. Equation 4 presumed that the area fraction was equal to the mass fraction (rather than the pressure fraction) of the compound.

The liquid mole fraction was unknown, so Equation 3b was solved for this variable with the result

$$\chi_I = \frac{\epsilon_I}{p_{VSATI}} \sum_I p_{VSATI}\chi_I \tag{5}$$

The ratio of a constituent I mole fraction to a second constituent (J) mole fraction followed simply from Equation 5

$$\frac{\chi_I}{\chi_J} = \frac{\epsilon_I}{p_{VSATI}} \cdot \frac{p_{VSATJ}}{\epsilon_J} \tag{6a}$$

$$\chi_I = \frac{\epsilon_I}{p_{VSATI}} \frac{p_{VSATJ}}{\epsilon_J} \chi_J \tag{6b}$$

A set of equations similar to 6b was constructed by holding J fixed while varying I over all the constituents. These equations were added together and solved for χ_J with the result

$$\chi_J = \frac{\epsilon_J}{p_{VSATJ}} \frac{\sum_I \chi_I}{\sum_I \frac{\epsilon_I}{p_{VSATI}}} \tag{7a}$$

$$\sum_I \chi_I = 0.42 \tag{7b}$$

The chromatographic area fractions from the headspace analysis were substituted into Equation 4 to compute ϵ_I, and the empirical

TABLE 1 GC/MS Headspace Analysis and Saturated Vapor Estimates[a]

Compound[b]	m_I, kg/mole	P_{VSATI}, ppm[c]	ε_I[d]	P_{VSI}, ppm	χ_I, %
2 Methylbutane	0.0722	755,000	0.035	500	0.0668
Pentane	0.0722	556,000	0.009	130	0.0244
2 Methylpentane	0.0862	225,000	0.152	2,230	0.995
3 Methylpentane	0.0862	201,000	0.088	1,260	0.631
Hexane	0.0862	159,000	0.134	1,970	1.25
Methylcyclopentane	0.0842	144,000	0.044	630	0.437
2 Methylhexane	0.100	67,600	0.074	1,070	1.58
2,3 Dimethylpentane	0.100	71,100	0.074	1,070	1.51
3 Methylhexane	0.100	63,200	0.044	640	1.02
2,2,4 Trimethylpentane	0.114	50,700	0.075	1,070	2.12
Heptane	0.100	46,200	0.018	260	0.570
Methylcyclohexane	0.0982	47,400	0.032	450	0.961
2,3,4 Trimethylpentane	0.114	27,300	0.022	320	1.17
2,3,3 Trimethylpentane	0.114	27,400	0.014	200	0.716
2,3 Dimethylhexane	0.114	23,400	0.034	490	2.09
2 Methylheptane	0.114	20,300	0.025	350	1.74
3 Methylheptane	0.114	19,300	0.034	490	2.53
2,2,4 Trimethylhexane	0.128	14,200	0.006	90	0.613
Octane	0.114	13,700	0.017	240	1.79
Ethylbenzene	0.106	9,350	0.008	100	1.11
p Xylene	0.106	8,550	0.016	210	2.45
Nonane	0.128	4,050	0.005	540	1.34
Propylbenzene	0.120	3,310	0.003	30	1.05
Trimethylbenzene	0.120	2,080	0.012	170	8.35
Decane	0.142	1,290	0.001	20	1.53

[a]Weathered petroluem liquid sample from MHD monitoring well, analyzed at 20°C.

[b]Compounds listed in elution order.

[c]P_{VSATI} values computed per Reid *(23)*.

[d]ε_I computed from gas chromatograph/mass spectrometer and Equation 4.

Equation 2 was used to estimate p_{VSATI}. The sum of volatile mole fractions $\sum_I \chi_I$ appearing in Equation 7b was estimated from a companion gc/ms estimate of the separate phase petroleum. The large number of compounds in the latter sample precluded precise estimates of individual mole fractions, however. The large amount of heavier hydrocarbon constituents implied by the χ_I values suggested that at least part of the petroleum spill consisted of diesel fuel or fuel oil (or both).

In view of Equation 1a and Table 1, the saturated headspace pressure was estimated to be

$$p_{VS} = 14{,}800 \text{ ppm} \qquad (293°K) \tag{8}$$

Saturated headspace standards at 293°K were injected into the portable gc in the field and the resulting total chromatographic area set equal to 14,800 ppm to calibrate the instrument response. In this way, the gc was used to corroborate the combustible hydrocarbon meter readings. Figure 4 (*left*) displays 21 oxygenated (>5 percent p_{VO}) Tedlar bag samples analyzed by both methods, agreement was reasonable over three orders of magnitude. Figure 4 (*right*) suggests that the ratio of gc to meter hydrocarbons increased with decreasing oxygen below the 5 percent level, presumably because of incomplete combustion in the catalytic chamber for hydrocarbon-rich, oxygen-poor soil gas. A calibrated empirical adjustment was accordingly applied to the organic vapor meter data

$$p_V = p_V(\text{meter})\left[C_7 + (C_8 - C_7)\frac{p_{VO}}{5}\right] \qquad (p_{VO} < 5\%) \tag{9a}$$

$$p_V = C_8\, p_V(\text{meter}) \qquad (p_{VO} > 5\%) \tag{9b}$$

$$C_7 = 2.83 \qquad (p_{VO} \text{ in } \%) \tag{9c}$$

$$C_8 = 0.905 \tag{9d}$$

Equation 9 is sketched as straight lines on Figure 4; the fitted C_8 value implies that the blend of petroleum hydrocarbon vapors burns more efficiently than the hexane used to calibrate the meter.

LATERAL PETROLEUM DISTRIBUTION AND BIODEGRADATION POTENTIAL

Table 2 and Figure 5 summarize depth-averaged soil gas vapor pressures for total hydrocarbon and oxygen observed in tubing clusters and vapor probe samples in the service area parking lot during the December 1993 and June 1994 field trips. A 10-m radius area

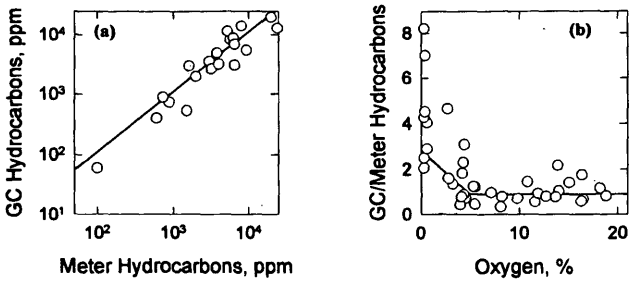

FIGURE 4 Combustible hydrocarbon meter and portable gas chromatogram data: *left*, oxygenated samples; *right*, gc/meter hydrocarbon readings versus oxygen content.

downgradient of the original tank pad contained saturated soil gas, with p_V values dropping off rapidly beyond a 20-m radius. Elevated hydrocarbons were found over the two separate phase contaminated MHD wells in the parking lot study area, which were gauged on May 13, 1994. Two other MHD wells without product were overlain by lower hydrocarbon vapor pressures.

The data were simply modeled to assess the aerobic biodegradation potential of the soil microbes. The hydrocarbon vapors were assumed to mineralize completely in accordance with the following reaction

$$C_7H_{16} + 11O_2 \xrightarrow{\text{microbes}} 7CO_2\uparrow + 8H_2O \tag{10a}$$

$$\gamma = 3.52 \tag{10b}$$

The assumed hydrocarbon molecular weight, m, of 0.10 kg/mole was close to the headspace average value of 0.0985 kg/mole; Equation 10a suggests that 3.52 kg of oxygen was required to degrade every kilogram of hydrocarbon, giving rise to the mass ratio γ cited in Equation 10b.

A radially symmetric, depth-averaged balance of presumably homogeneous diffusion and reaction was taken to describe the variation of hydrocarbon H and oxygen O vapor concentrations

$$-\frac{D_H}{r}\frac{d}{dr}\left(r\frac{dH}{dr}\right) - k(H_S - H) = -V \qquad (r < R) \tag{11a}$$

$$H = 0 \qquad (r > R) \tag{11b}$$

$$-\frac{D_O}{r}\frac{d}{dr}\left(r\frac{dO}{dr}\right) = -\gamma V \qquad (r < R) \tag{11c}$$

$$-\frac{D_O}{r}\frac{d}{dr}\left(r\frac{dO}{dr}\right) = 0 \qquad (R < r < R_A) \tag{11d}$$

$$O = O_A \qquad (R_A < r) \tag{11e}$$

where

r = radial distance,
H_S = saturated hydrocarbon vapor concentration, and
D_H, D_O = hydrocarbon and oxygen gaseous diffusivities, respectively.

A first-order source term with strength k modeled the evaporation of liquid petroleum from the source radius R into the unsaturated zone. A zero-order reactive term V was assumed, predicated on the abundance of the electron acceptor oxygen and the electron donor hydrocarbon. Hydrocarbon vapors and the degradation reaction were assumed to be negligibly small beyond the separate phase petroleum source, and the oxygen vapors were assumed to attain a background value O_A at radius R_A. The molecular diffusivities were assumed (*24*) to be given by

$$D_H = 2.50 \times 10^{-6}\,\frac{m^2}{s} \tag{12a}$$

$$D_O = 1.77 D_H \tag{12b}$$

The higher oxygen diffusivity cited in Equation 12b reflected the inverse dependence of diffusivities on molecular weight (*23*).

TABLE 2 Borehole Averaged Soil Vapor Pressures and Radial Distances

Designation	Depths	Date	p_{VO}, %	p_V, ppm	r,[a]
Probe 1	2	28Dec93	3.6	31,800[b]	9.54
Probe 2	2	28Dec93	9.8	13,800[b]	2.64
Probe 3	6	28Dec93	11.9	4,440[c]	14.8
Probe 4	3	28Dec93	8.0	180[c]	27.0
Probe 5	2	28Dec93	11.4	140[c]	21.7
Probe 6	1	28Dec93	13.9	11,300[b]	13.5
Probe 7	1	28Dec93	2.8	12,900[b]	13.9
Probe 9	2	1Jun94	15.8	1,670[b]	16.0
Probe 10	11	1Jun94	17.8	110[c]	31.1
Probe 11	12	1Jun94	2.2	4,500[c]	15.6
Probe 12	10	1Jun94	3.0	7,530[c]	11.9
Probe 13	1	1Jun94	13.7	3,130[b]	23.5
Probe 14	10	1Jun94	13.7	100[c]	22.9
Probe 18	9	3Jun94	15.8	200[c]	27.2
Probe 19	12	3Jun94	3.6	11,400[c]	23.2
Cluster 1AA	2	2Jun94	5.2	190[c]	34.2
Cluster 2AC	4	11Jul94	1.3	11,800[b]	6.32
Cluster 2AA	3	11Jul94	2.0	20,700[b]	10.2
Cluster 3AA	3	2Jun94	9.3	100[c]	36.2
Cluster 7AA	3	1Jun94	7.4	120[c]	16.3
Cluster 7AB	1	11Jul94	4.3	2,300[b]	21.3
Cluster 12AB	1	2Jun94	11.2	90[c]	28.3
Cluster 14AA	1	2Jun94	13.5	90[c]	27.0
Cluster 16AA	2	2Jun94	17.3	80[c]	47.7
Cluster 16AC	4	2Jun94	15.6	80[c]	59.1

[a]Distance from equivalent source origin, sketched in Figure 5.

[b]Measured with gas chromatograph.

[c]Measured with total hydrocarbon meter and adjusted in accordance with Equation 9.

The equidimensional differential equation for oxygen and the Bessel equation for hydrocarbons (*25*) yielded the following solution

$$H = \left(H_S - \frac{V}{k}\right)\left\{1 - \frac{I_0\left[r\left(\frac{k}{D_H}\right)^{1/2}\right]}{I_0\left[R\left(\frac{k}{D_H}\right)^{1/2}\right]}\right\} \qquad (r < R) \qquad (13a)$$

$$O = \frac{\gamma V r^2}{4D_O} \qquad (r < R) \qquad (13b)$$

$$O = \frac{\gamma V R^2}{2D_O}\left[\frac{1}{2} + \ln\left(\frac{r}{R}\right)\right] \qquad (r > R) \qquad (13c)$$

with modified Bessel function of the first kind of order zero I_0. Equation 13c ensured continuous oxygen and oxygen fluxes at the

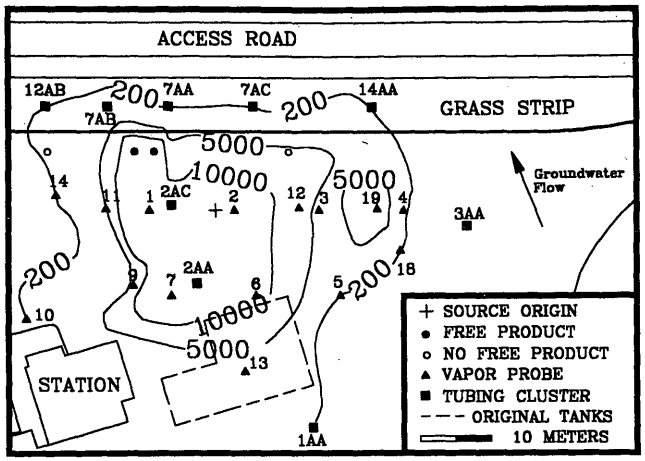

FIGURE 5 Depth-averaged total hydrocarbon vapor pressure isopleths (ppm) and equivalent source origin.

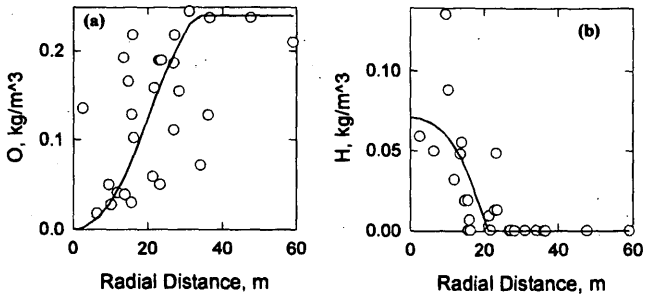

FIGURE 6 Observed (symbols) and calibrated (curves) soil vapor profiles: *left*, oxygen concentrations; *right*, total hydrocarbon concentrations.

edge of the hydrocarbon spill, and Equation 13a was consistent with Equation 11b. The hydrocarbon vapor profile was also finite at the source origin.

A Fibonnaci search was conducted to fit Equations 13b and 13c to the borehole averaged oxygen data for an assumed source radius R of 20 m and a source origin sketched on Figure 5, with radial distances cited in Table 2. The ideal gas law (*22*) was used to convert gaseous partial pressures to concentrations

$$O = \frac{p_{VO}\, m_O}{R_U\, T} \qquad (m_O = 0.032 \text{ kg/mole}) \tag{14a}$$

$$H = \frac{p_V\, m}{R_U\, T} \qquad (m = 0.100 \text{ kg/mole}) \tag{14b}$$

$$R_U = 8.31\ \frac{\text{Pa} - m^3}{\text{mole} - {}^\circ\text{K}} \tag{14c}$$

where R_U is the universal gas constant and m_O is the molecular weight of oxygen. The maximum reaction rate was varied to minimize the model error standard deviation with the results given by

$$V = 1.54 \times 10^{-9}\ \frac{\text{kg}}{m^3 - s} \tag{15}$$

Figure 6 (*left*) displays the calibration and oxygen data. The saturated hydrocarbon vapor concentration and the source strength were fit to the hydrocarbon data with the following result

$$H_S = 0.127\ \frac{\text{kg}}{m^3} \tag{16a}$$

$$k = 5.98 \times 10^{-8}\ s^{-1} \tag{16b}$$

Figure 6 (*right*) shows the hydrocarbon data, computed from Table 2 and the ideal gas law, and the model calibration. It is important to note that the oxygen and hydrocarbon models were coupled through the stoichiometry of a common reactive term. The observed trend of increasing oxygen and decreasing hydrocarbon vapor concentrations with distance away from the origin was recovered by the model. Physically speaking, petroleum constituents diffuse radially away from the center of contamination. This origin also serves as a biological sink due to aerobic degradation, so that oxygen diffuses toward the center.

DISCUSSION OF RESULTS

Ostendorf et al. (*24*) analyzed aviation gasoline evaporation out of intact core samples from an Environmental Protection Agency (EPA) field research site with a detailed data base and mathematical model. The evaporative source strength k^* from that model was equated to the present source term with the theoretical result

$$k \approx \frac{k^* L}{10b} \tag{17}$$

where L is the thickness of the contaminated soil and b is the thickness of the unsaturated zone. The aviation gasoline source strength k^* varied from 10^{-6} to $10^{-5}\ s^{-1}$ in the EPA cores. This range, along with a parking lot L/b estimate of 0.1, were inserted into Equation 17 to get a k range of 10^{-8} to $10^{-7}\ s^{-1}$, which compared favorably with Equation 16b. Richards et al. (*26*) measured maximum reaction rates in soil microcosms from the 4.5-m depth in soil at the EPA research site. The soil microbes degraded a blend of alkane and aromatic vapors representative of aviation gasoline under aerobic conditions, and a V of about 2×10^{-9} kg/m^3-s was observed. This value, which compares reasonably well with Equation 15, is an order of magnitude smaller than the V-levels near the ground surface at the EPA site. The calibrated H_S value (Equation 16a) is considerably higher than the headspace value of 0.0306 kg/m^3 implied by Table 1 constituents at a soil temperature of 281.6°K; it is likely that volatile fractions are underrepresented in Table 1 because of weathering of the separate phase standard during storage.

The hydrocarbon evaporation rate F_E out of the separate phase petroleum was estimated from the calibrated source strength and saturated concentration (Equation 16)

$$F_E = \pi R^2\, b\theta_A\, kH_S \tag{18a}$$

$$F_E = 6.18 \times 10^{-6}\ \frac{\text{kg}}{s} \tag{18b}$$

with an unsaturated zone thickness of 2.5 m. A measured petroleum density of 810 kg/m^3, in view of Equation 18b, implied a natural evaporative diffusion of 63 gal/year from the service area parking lot.

Further model refinements for transience, heterogeneity, measured degradation kinetics, density-driven advection, sorption, and the actual source distribution implied by separate phase coring data would doubtless reduce the scatter of the data about the calibrated curves of Equation 5. MHD and UMASS researchers are pursuing a program consisting of tubing cluster monitoring, solid core sampling, and soil microcosm studies to document these model improvements and improve the estimates of evaporation, degradation, and distribution of soil gas constituents. Nonetheless, the simple analysis and sparse data of Table 2 suggest that aerobic degradation occurs naturally in the subsurface of the parking lot. Furthermore, the separate phase petroleum under the lot is likely to be confined to a 20-m radius centered downgradient of the original storage tanks. The preponderance of diesel range organic constituents suggests that at least part of the spill is diesel or fuel oil.

Equipment and labor costs are associated with this delineation of a petroleum spill and preliminary assessment of its remediation potential. Basic field equipment needed for an elementary soil gas survey include the following items (with 1994 cost estimates cited): (*a*) total hydrocarbon vapor meter ($2,500), (*b*) soil gas oxygen analyzer ($1,500), and (*c*) electric hammer ($1,500). Commercial kits containing drill rods and vapor probes are available for about $1,000, but caution should be exercised when deploying these systems in compacted soils or cobble layers. A rig-driven hammer with thicker rods and customized probes may be needed under these adverse conditions, which are likely to be encountered in the compacted soils of highway rights of way. The labor associated with soil gas sampling depends largely on the character of the unsaturated zone as well. If drill rigs are required, it is possible to profile 10 depths at one vapor probe location each hour under favorable conditions, using a two-person rig crew and a three-person sampling team. Lower labor and a more rapid sampling rate are required for manually driven probes in less resistive soil.

The meter-based technology, with its reasonable costs and a modest level of training, yields qualitative distributions of total hydrocarbon and oxygen partial pressures in the soil gas. The abrupt drop of hydrocarbon levels signals the lateral extent of underlying liquid petroleum contamination, whereas the coincidence of high hydrocarbon and low oxygen concentrations implies an aerobic biodegradation potential. Further quantitative conclusions require more elaborate equipment (gas chromatographs) and sophisticated laboratory analysis (gc/ms).

CONCLUSIONS

The lateral distribution, approximate composition, and aerobic biodegradation potential of vapors from a petroleum hydrocarbon spill in an MHD right of way were inferred from soil gas sampling technology and analyses. Stainless steel vapor probes and stainless steel tubing clusters yielded Tedlar bag samples for on-site analysis by a combustible hydrocarbon meter, an oxygen analyzer, and a portable gas chromatograph. The hydrocarbon data delineated the horizontal extent of the petroleum spill and, with the observed oxygen, calibrated a simple coupled transport model that confirmed the aerobic biodegradation potential of naturally occurring microbes in the site soil.

ACKNOWLEDGMENTS

This research was funded as a task order of the Transportation Research Program, an interagency service agreement between MHD and the University Transportation Center of the University of Massachusetts at Amherst. The authors acknowledge and appreciate the work of UMASS research assistants Erich Hinlein, Paul Cheever, Russ Suchana, and Pierre Tehrany along with the logistical support provided by District 4 personnel of MHD.

REFERENCES

1. Deyo, B. G., G. A. Robbins, and G. K. Binkhorst. Use of Portable Oxygen and Carbon Dioxide Detectors To Screen Soil Gas for Subsurface Gasoline Contamination. *Groundwater*, Vol. 31, No. 4, July–August 1993, pp. 598–604.
2. Downey, D. C., and P. H. Guest. Physical and Biological Treatment of Deep Diesel Contaminated Soils. *Proc., Petroleum Hydrocarbons and Organic Chemicals in Groundwater*, National Groundwater Association/American Petroleum Institute, Dublin, Ohio, 1991, pp. 361–376.
3. Folkes, D. J., M. S. Bergman, and W. E. Herst. Detection and Delineation of a Fuel Oil Plume in a Layered Bed Rock Deposit. *Proc., Petroleum Hydrocarbons and Organic Chemicals in Groundwater*, National Groundwater Association/American Petroleum Institute, Dublin, Ohio, 1987, pp. 279–304.
4. Marrin, D. L. Soil Gas Sampling and Misinterpretation. *Groundwater Monitoring Review*, Vol. 8, No. 2, Spring 1988, pp. 51–54.
5. Van Vliet, D. J., N. R. Thomson, and J. F. Sykes. Seasonal Concentration Fluctuation of Volatile Organic Compounds in the Subsurface. *Proc., Petroleum Hydrocarbons and Organic Chemicals in Groundwater*, National Groundwater Association/American Petroleum Institute, Dublin, Ohio, 1993, pp. 577–591.
6. Ostendorf, D. W., and D. H. Kampbell. Biodegradation of Hydrocarbon Vapors in the Unsaturated Zone. *Water Resources Research*, Vol. 27, No. 4, April 1991, pp. 453–462.
7. Kerfoot, H. B., C. L. Mayer, P. B. Durgin, and J. J. D'Lugosz. Measurement of Carbon Dioxide in Soil Gases for Indication of Subsurface Hydrocarbon Contamination. *Groundwater Monitoring Review*, Vol. 8, No. 2, Spring 1988, pp. 67–71.
8. Marrin, D. L. Subsurface Biogenic Gas Ratios Associated with Hydrocarbon Contamination. *Proc., In Situ Bioreclamation*, Butterworth-Heinemann, Boston, Mass., 1991, pp. 546–560.
9. Miller, R. N., C. C. Vogel, and R. E. Hinchee. A Field Scale Investigation of Petroleum Hydrocarbon Biodegradation in the Vadose Zone Enhanced by Soil Venting at Tyndall AFB, Florida. *Proc., In Situ Bioreclamation*, Butterworth-Heinemann, Boston, Mass., 1991, pp. 283–302.
10. Kittel, J. A., R. E. Hinchee, R. N. Miller, C. C. Vogel, and R. Hoeppel. In Situ Respiration Testing: A Field Treatability Test for Bioventing. *Proc., Petroleum Hydrocarbons and Organic Chemicals in Groundwater*, National Groundwater Association/American Petroleum Institute, Dublin, Ohio, 1993, pp. 351–366.
11. Kampbell, D. H., J. T. Wilson, and D. W. Ostendorf. Simplified Soil Gas Sensing Techniques for Plume Mapping and Remediation Monitoring. *Proc., 3rd National Conference on Petroleum Contaminated Soils*, Lewis Publishers, Chelsea, Mich., 1990, pp. 125–139.
12. Kerfoot, H. B. Soil Gas Measurement for Detection of Groundwater Contamination by Volatile Organic Compounds. *Environmental Science and Technology*, Vol. 21, No. 10, Oct. 1987, pp. 1022–1024.
13. Christy, T. M., and S. C. Spradlin. The Use of Small Diameter Probing Equipment for Contaminated Site Investigation. *Proc., 6th National Outdoor Action Conference*, National Groundwater Association, Dublin, Ohio, 1992, pp. 87–101.
14. Tillman, N., and L. Leonard. Vehicle Mounted Direct Push Systems, Sampling Tools, and Case Histories: An Overview of an Emerging Technology. *Proc., Petroleum Hydrocarbons and Organic Chemicals in Groundwater*, National Groundwater Association/American Petroleum Institute, Dublin, Ohio, 1993, pp. 177–188.
15. Moyer, E. E., D. W. Ostendorf, D. H. Kampbell, and Y. F. Xie. Field Trapping of Subsurface Vapor Phase Petroleum Hydrocarbons. *Groundwater Monitoring and Remediation*, Vol. 14, No. 1, Winter 1994, pp. 110–119.
16. Robbins, G. A., B. G. Deyo, M. R. Temple, J. D. Stuart, and M. J. Lacy. Soil Gas Surveying for Subsurface Gasoline Contamination Using Total Organic Vapor Detection Instruments 1. Theory and Laboratory Exper-

imentation. *Groundwater Monitoring Review*, Vol. 10, No. 3, Summer 1990, pp. 122–131.
17. Potter, T. L. Analysis of Petroleum Contaminated Soil and Water: An Overview. *Proc., 2nd National Conference on Petroleum Contaminated Soils*, Lewis Publishers, Chelsea, Mich., 1989, pp. 97–109.
18. Massachusetts Highway Department. *Hydrogeologic Investigation MHD Service Station*. Groundwater Technology, Inc., Norwood, Mass., 1988.
19. Massachusetts Highway Department. *Environmental Site Assessment Report*. Hidell-Eyster Technical Services, Inc., Boston, Mass., 1987.
20. Massachusetts Highway Department. *Groundwater Remediation Plan*. Groundwater Technology, Inc., Norwood, Mass., 1988.
21. Massachusetts Highway Department. *Evaluation of Existing Petroleum Recovery System*. HMM Associates, Inc., Concord, Mass., 1991.
22. Eastman, R. H. *Essentials of Modern Chemistry*. Rinehart Press, San Francisco, Calif., 1975.
23. Reid, R. C., J. M. Prausnitz, and B. E. Poling. *The Properties of Gases and Liquids*. McGraw-Hill, New York, 1987.
24. Ostendorf, D. W., E. E. Moyer, Y. F. Xie, and R. V. Rajan. Hydrocarbon Vapor Diffusion in Intact Core Sleeves. *Groundwater Monitoring and Remediation*, Vol. 13, No. 1, Winter 1993, pp. 139–150.
25. Hildebrand, F. B. *Advanced Calculus for Applications*. Prentice-Hall, Englewood Cliffs, N.J., 1976.
26. Richards, R. J., D. W. Ostendorf, and M. S. Switzenbaum. Aerobic Soil Microcosms for Long-Term Biodegradation of Hydrocarbon Vapors. *Hazardous Waste and Hazardous Materials*, Vol. 9, No. 4, 1992, pp. 397–410.

The views, opinions, and findings contained in this paper are those of the authors and do not necessarily reflect the official view or policy of the MHD. This paper does not constitute a standard, specification, or regulation.

Publication of this paper sponsored by Task Force on Waste Management in Transportation.